Journal of Theoretical and Applied Vibration and Acoustics 5(2) 131-152 (2019)

I S A V

Journal of Theoretical and Applied Vibration and Acoustics

journal homepage: http://tava.isav.ir

Nonlinear lap joint interface modeling and updating strategies for assembled structures

Ehsan Shahabi, Hamid Ahmadian*

Center of Excellence in Experimental Solid Mechanics and Dynamics, School of Mechanical Engineering, Iran University of Science and Technology, Narmak, Tehran 16844, Iran

ARTICLE INFO

Article history:
Received 8 September 2019

Received in revised form
30 October 2019

Accepted 23 November 2019

Available online 11 December 2019

Keywords:
Lap joint interface,

Friction contact,

Thin layer interface,

Zero thickness element,

Nonlinear frequency response.

ABSTRACT

A comparison between two known strategies of modeling lap joint interfaces, namely, zero-thickness and thin layer interface theories and their associated updating procedures, is made. Finite element models capable of accurately representing nonlinear behavior of assembled structures with localized nonlinearities in their bolted lap joint are developed. A practical strategy is employed in updating of these structures that initially parameters describing linear behavior are updated based on the low-amplitude excitation experimental observations. In the next step, parameters representing nonlinear effects are updated using stepped-sine excitations near the structure resonance frequency. In both steps, the Particle Swarm Optimization (PSO) algorithm is used to reduce the discrepancies between experimental observations and model predictions. The identified contact interface models are validated by comparing their predictions with the experimental data not included in the updating procedure. In what concerns the updating process, the convergence rate of parameter identification in a model with zero thickness frictional contact elements was lower and more time-consuming compared to the model with thin layer interfaces. This study shows assigning appropriate material properties for the thin interface layer results in contact forces with comparable accuracy to the ones obtained by zero thickness elements with less computational efforts.

* Corresponding author:
E-mail address: ahmadian@iust.ac.ir (H. Ahmadian)

http://dx.doi.org/10.22064/tava.2020.127915.1168

Nomenclature

c	decay coefficient	σ	normal stress
E	Young modulus	τ	shear stresses
G	Shear modulus	μ	coefficient of friction
f	natural frequency	ε	normal strain
K	contact stiffness	γ	shear strain
N	normal load	Subscripts	
S_y	yield stress	t	tangential direction
T	Tangential force	n	normal direction
u	directional displacement	e	elastic
$\dot{w}$	slipping velocity	p	plastic

1. Introduction

Modeling mechanical joints capable of estimating the dynamic response of assembled structures is a crucial step in the structural design and analysis process. At high excitation amplitudes, contacts behave in a nonlinear manner and produce softening effects and added damping. In these circumstances neglecting the nonlinear behavior of contacts may lead to incorrect response predictions. Thus presenting accurate and reliable models for the mechanical contacts is of particular importance. Joint interfaces produce features such as softening effects in the structure at higher excitation levels and dissipate energy. The energy dissipation reduces vibration, and resultant noise is omitted from the system. The mechanisms that cause damping in the joints can be divided into the slip and vibro-impact categories, where the latter mechanism may become a new noise source in some circumstances. The energy dissipation rate in each of these two mechanisms depends on geometry, material properties, surface roughness, preload, and also the excitation nature.

Studies about modeling joints started decades ago and are continuing. Researchers have adopted two different approaches for modeling the joints behavior using parametric and nonparametric models. In the first approach, predetermined mathematical models with unknown parameters are used, and the purpose is to identify appropriate values for these parameters. In this approach, in order to select a suitable mathematical model, acquiring sufficient knowledge of physical phenomena in the joint is of particular importance. Researchers have conducted many experimental studies in order to determine precisely the physical phenomena in the joints [1-3]. In particular, a method for identifying the joint interface stiffness model representing physical parameters of the contact interfaces, such as surface roughness and preload effects, is discussed by Jalali *et al* [4].

In a second approach, a search in function spaces is performed in order to choose an appropriate structure for modeling mechanical joint effects. In other words, in this approach to model the joint interface behavior, a pre-assumed structure is not used, but the stiffness and damping effects of the mechanical joint in the model are studied and identified as unknown external forces [5, 6]. The nonlinear effects in structures such as friction in contacts can be modeled with the aid of force state mapping. In this method, restoring force is defined using the nonlinear parameter as a function of the system states.

In finite element modeling, there are two conventional methods for modeling mechanical joint interfaces, namely employing thin layer interface elements and zero thickness element models. In thin layer theory, the contact between two parts is modeled with a thin layer of virtual material that behaves similarly to the stiffness and damping of the contact interface. Thin layer theory is employed in the dynamic modeling of assembled structures by many researchers [7, 8]. Ahmadian *et al.*[9, 10] used thin layer theory with elastoplastic material for modeling the nonlinear surface-to-surface contact interface. Alamdari *et al.*[11] considered Richard-Abbot elastic-plastic material for characterizing energy dissipation and softening phenomena in a joint at a nonlinear state. They proposed a thin layer of elements with virtual material properties at the joint location to present its nonlinear behavior in the tangential direction.

Several models representing mechanical contacts using zero thickness elements are also presented. Iwan contact model is widely used for simulating the contact interface hysteretic behavior via combinations of serial and parallel springs-sliders [12]. Lacayo *et al.* [13] conducted a numerical study to demonstrate the limitations of modal Iwan models. Lacayo and Allen [14] later updated parameters of an Iwan's model, suggested primarily for predicting micro and macro slip behavior of bolted joints, using a quasi-static algorithm. Abad *et al.*[15] used the Valanis model to represent frictional contacts in a structure in order to simulate its dynamic behavior. Segalman [16] presented FE models based on material plasticity, including Jenkins and Iwan models. Berger [17] introduced a wide range of different models, which can predict micro slip, partial slip, and passive damping behaviors in the contact. Ahmadian *et al*[18]. developed a nonlinear generic element formulation for simulating the behavior of a bolted joint. Jalali-Mashayekhi and Kövecses.[19] used the augmented Lagrangian based formulations to deal with non-smooth contact models. Stadler[20] proposed a first-order augmented Lagrange method for determining the contact interface forces. Also, Stupkiewicz *et al*. [21]. showed that the augmented Lagrange method is appropriate for sensitivity analysis in the solution of frictional contact joints.

Several attempts have been made during recent years for modeling the bolted joints in structure, and researchers have used different FE codes [22, 23]. While many researchers and practitioners have worked on planar lap-joint contacts, this paper investigates the dynamic behavior of cylindrical lap-joint contacts due to its frequent use in tabular tower structures and fluid transfer lines. In this paper, a thin layer interface and zero-thickness models are employed to represent a cylindrical bolted lap joint. In the former model, the bolted lap joint contact interface is represented using a thin layer of solid elements with virtual material properties. For the second method, modeling of the contact area is performed using frictional contact elements. The parameters of these models are identified using experimental observations. Zero thickness elements are employed in modeling contact interfaces with a variety of nonlinear effects such as micro/macro slip, vibro-impacts, and slapping. However, their associated multi-rule constitutive equations require costly and time-consuming computations. This paper shows by the appropriate selection of material properties of a thin layer interface, a model with comparable accuracy to the one obtained by zero thickness elements is achieved. However, it is notable that the model with a thin layer interface requires less computational efforts in determining the assembled structure response under any loading excitation compared to the one employed zero thickness elements. Models involving zero thickness elements produce ordinary differential equations that are numerically stiff and, therefore, computationally cumbersome.

The present paper is organized as follows. Section 2 considers zero thickness frictional element formulation and thin layer element theory. In Section 3, an experimental study is presented consisting of a cylindrical structure assembly with a cylindrical bolted lap joint in the middle. The excitation of the structure was performed at different excitation levels to observe linear and nonlinear behaviors of the structure. In section 4, experimental results are employed to update FE models and to obtain the zero-thickness and thin layer contact parameters. Section 5 is dedicated to verification of the updated FE models in predicting the measured frequency responses and hysteresis loops and evaluates the performance of each strategy in describing the contact interface effects. Finally, section 6 provides some concluding remarks.

2. Joint contact interface

This section provides theoretical bases for modeling contacts in proceeding finite element analysis and model updating. Both scenarios of zero-thickness and thin layer interface modeling are discussed, and formulations used in modeling the test structure contact interfaces are provided.

2.1. Frictional contact element

Coulomb friction model is used in modeling frictional contacts similar to the one shown in Figure 1 to define the contact between each set of opposing nodes in a lap joint interface. Each zero thickness contact element, also called 2D Jenkins element, is composed of a slider in series with two orthogonal shear springs K_{t1} and K_{t2} while a variable normal load is applied on the slider using the stiffness K_n,

$$T_i = K_{ti} u_i, \quad i = 1,2, \tag{1}$$

$$N = N_0 + K_n u_3, \tag{2}$$

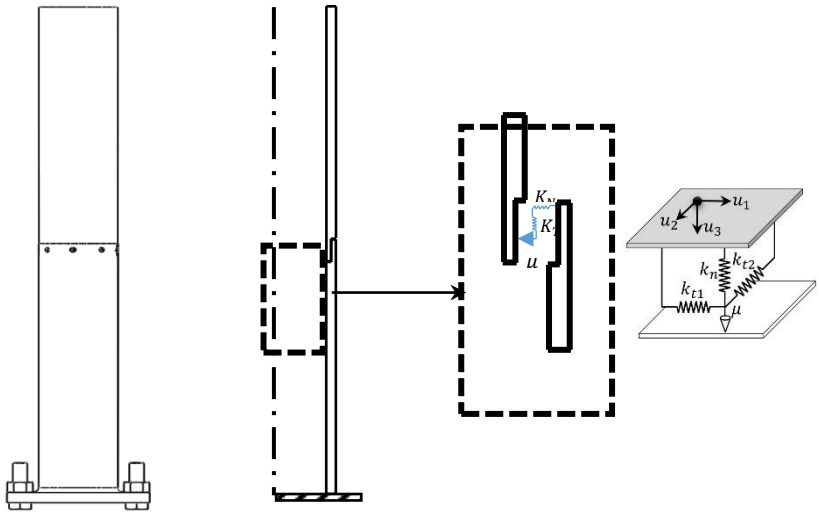

Fig. 1: Cylindrical bolted lap joint model, frictional contact element

where u_i is the relative displacement between contacting nodes and N_0 is their contact normal preload. In the sticking mode the equivalent shear force in the sliding plane, T, is less than limit frictional force μN, and no-slip occurs between the surfaces,

$$T = \sqrt{T_1^2 + T_2^2} \leq \mu N. \tag{3}$$

Slippage occurs between two surfaces when the shear force overcomes the friction force between contacting surfaces. When the frictional force equals μN, the target and contact surfaces move relative to each other and sliding occurs along slipping velocities $\dot{w}_i$, $i = 1,2$,

$$\begin{Bmatrix} T_1 \\ T_2 \end{Bmatrix} = \frac{\mu N}{\|\dot{w}\|} \begin{Bmatrix} \dot{w}_1 \\ \dot{w}_2 \end{Bmatrix}, \|\dot{w}\| = \sqrt{\dot{w}_1 + \dot{w}_2}. \tag{4}$$

Many commercial FE codes employ penalty methods such as those employed by Abad *et al.*, [24] and Qin *et al*.[25]in an iterative manner to update the contact states, i.e., shear and normal forces and their corresponding displacement fields. In a frictional element model, separation of contacting surfaces may occur when both normal and in-plane shear forces are equal to zero.

When relative motion occurs between contact surfaces, the friction coefficient between the surfaces reduces and becomes a function of slippage velocity. Changing trend and the behavior of velocity-dependent friction coefficient function, $\mu(\dot{w})$, is defined by various friction models. A review of the models that simulate this trend is provided by Pennestri *et al.* [26] including the exponential friction model,

$$\mu(\dot{w}) = \mu_D + (\mu_s - \mu_D)e^{-c\|\dot{w}\|}. \tag{5}$$

The exponential friction coefficient function is expressed in terms of static, μ_s, and dynamic, μ_D, friction coefficients plus a decay coefficient *c*.

In this study, the contact is modeled using a series of parallel zero thickness frictional elements in which connect opposing nodes in the lap joint interface. The created interface model with a large number of Jenkins elements may be regarded as a distributed Iwan model. In a distributed lap joint, the relative normal displacement between opposing nodes, u_3, are different in each area, which creates a varying normal force in the interface surface. Variations of normal forces allow slippage in some parts of the interface with a low normal load while areas with higher normal loads are in stiction.

2.2.The joint interface layer theory

A thin layer of virtual elastoplastic material is also employed to simulate the contact behaviors such as bolted joints shown in Figure 2. The driving objective in employing thin layer interface elements is their low computational efforts required to estimate contact forces compared with the zero-thickness elements. This study shows by carefully parameterizing the constitutive law of thin layer interface material, a computationally more efficient model compared to the one obtained with zero-thickness elements is achieved.

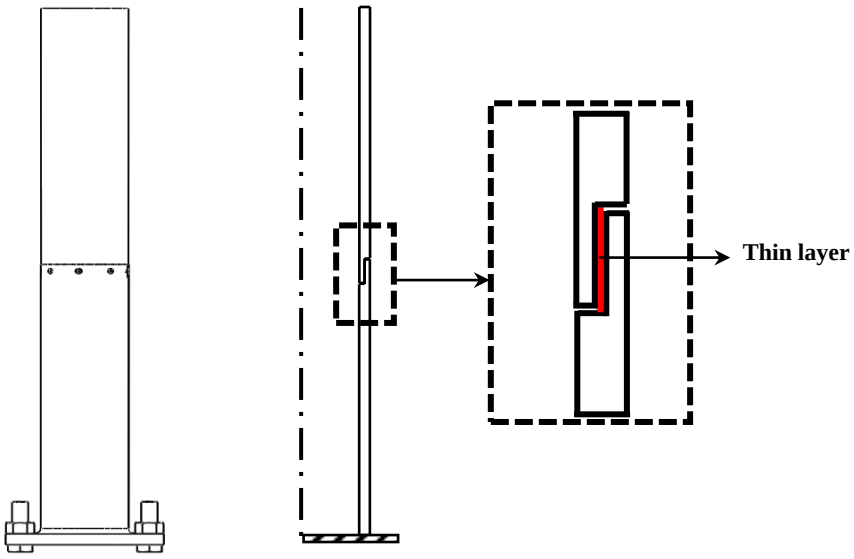

Fig. 2: Cylindrical bolted lap joint model, the thin layer model

In this approach, which initially was presented to model interfaces between rocks [27], the joint interface is modeled with continuous elements of finite thickness. The thin layer virtual material provides similar stiffness properties of the joint contact, which governs its behavior under static and dynamic loadings. The virtual material constitutive equation considers elastic deformations at the contact stick state, and plastic deformations represent slippage in the contact. An important issue in applying the thin layer theory is selecting their aspect ratios. Pande and Sharma [28] state as long as there is an appropriate element formulation, it is possible to employ elements with large aspect ratios without substantial numerical errors. When a bolted joint is placed under a tension leading to tangential loading, it experiences three load-displacement states of stick, micro-slip, and macro-slip. For a joint which behaves linear-elastic, the constitutive relationship can be expressed as,

$$\begin{cases} \Delta\sigma = K_n \Delta u_3 \\ \Delta\tau_1 = K_t \Delta u_1 \\ \Delta\tau_2 = K_t \Delta u_2 \end{cases} \tag{6}$$

where $\Delta\sigma, \Delta\tau_1$and $\Delta\tau_2$ are the elastic parts of the incremental normal and tangential stresses and $\Delta u_3, \Delta u_1$ and Δu_2 are the incremental relative normal and tangential displacements across the joint, respectively. It is worth mentioning that the subscripts '1' and '2' indicate the two orthogonal tangential directions in the contact plane and also the parameters $K_n$and $K_t = K_{t1} = K_{t2}$ are coefficients which penalize surface penetration and slipping, respectively. When the elastic load limit of a joint is higher than the allowance limit, the joint behavior follows an elastic-plastic law. In this situation, the state of sliding can be presented by a quasi-linear constitutive equation at each increment.

The joint behaves linearly in the sticking state and nonlinear in the micro and macro-slip states. In thin layer theory, the joint's nonlinear behavior is modeled via related nonlinear stress-strain relations. The stress-strain relation for virtual material of the contact layer is implemented using a general form of the constitutive model as,

$$\begin{Bmatrix}\sigma_{11}\\ \sigma_{22}\\ \sigma_{33}\\ \tau_{12}\\ \tau_{23}\\ \tau_{31}\end{Bmatrix} = \begin{bmatrix} C_{11} & C_{12} & C_{13} & C_{14} & C_{15} & C_{16} \\ & C_{22} & C_{23} & C_{24} & C_{25} & C_{26} \\ & & C_{33} & C_{34} & C_{35} & C_{36} \\ & & & C_{44} & C_{45} & C_{46} \\ & & & & C_{55} & C_{56} \\ Sym. & & & & & C_{66} \end{bmatrix} \begin{Bmatrix}\varepsilon_{11}\\ \varepsilon_{22}\\ \varepsilon_{33}\\ \gamma_{12}\\ \gamma_{23}\\ \gamma_{31}\end{Bmatrix}. \tag{7}$$

The virtual material constitutive equations of the interface layer are defined using 21 unknown parameters. Mayer and Gaul [29] assume off-diagonal terms are negligible, $C_{11}$and C_{22} terms are also omitted as in-plane stiffness of joint interface is not considered in modeling. Also twisting of the interface element is of no interest, therefore, the term C_{44} is omitted. There remains, C_{33} as the normal stiffness in the joint interface and C_{55} and C_{66} are tangential stiffness where in stick state $C_{33} = E$ and $C_{55} = C_{66}$=G.

A bolted joint under tangential loading demonstrates three states of sticking, micro, and macro-slip. Simulation of behavior of bolted joint in these three states, which involves a transition from linear to nonlinear behavior is described using a thin layer of elastoplastic material. This nonlinear behavior is modeled by nonlinear stress-strain relation of the contact zone. In this investigation, assuming isotropic properties for the virtual material, constitutive equation of the contact zone thin layer is adopted as:

$$C_{33} = E_p + \left(E_e - E_p\right)\left(1 + \left(\frac{\left|\left(E_e - E_p\right)\varepsilon_{33}\right|}{S_y}\right)^n\right)^{-\left(\frac{1}{n}\right)}, \tag{8a}$$

$$C_{55} = C_{66} = \nu\, C_{33}, \tag{8b}$$

where, E_e is vitrtual marerial Young's modulus, E_p is tangent modulus, S_y is yield stress, ν is Poisson's ratio, and n defines the smoothness of transition curvature from stick to macro-slip behavior. Each part of the interface layer, depending on the local strain ε_{33}, may behave in stick, miro-slip, or macro-slip.

3. Experimental case study

The test structure consists of two cylindrical shells connected using eight M4 bolts and nuts. Bolts are equally spaced circumferentially and connect the two cylindrical parts. The cylindrical parts were made from a steel pipe, and lap joint contact surfaces were manufactured in each part using the machining process. The contact interface of the test structures was designed to exhibit a variety of features that are common in practice. These features include:

a) a distributed contact interface with varying preload where interface regions close to the bolts experience high preload and the normal contact stiffness becomes weak in regions far from the bolts, and

b) micro/macro slip phenomena occur in the various regions of the interface depending on the external excitation load level and the local preload of the contact region.

The geometric specifications of the structure are shown in Figure 3. Part B of the structure is welded to a base plate grounded by four M20 bolts.

3.1. Impact hammer tests

First, to make sure the base plate bolts provide stiff elastic support with no slippage at this support within the range of applied excitation loads, substructure B was excited at point D using an instrumented hammer, and the response was recorded in point E as indicated in Figure 3. The excitation force levels in testing sub-structure B was kept higher than any proceeding tests to ensure there was no slippage in the assembled structure clamping support in the following excitations.

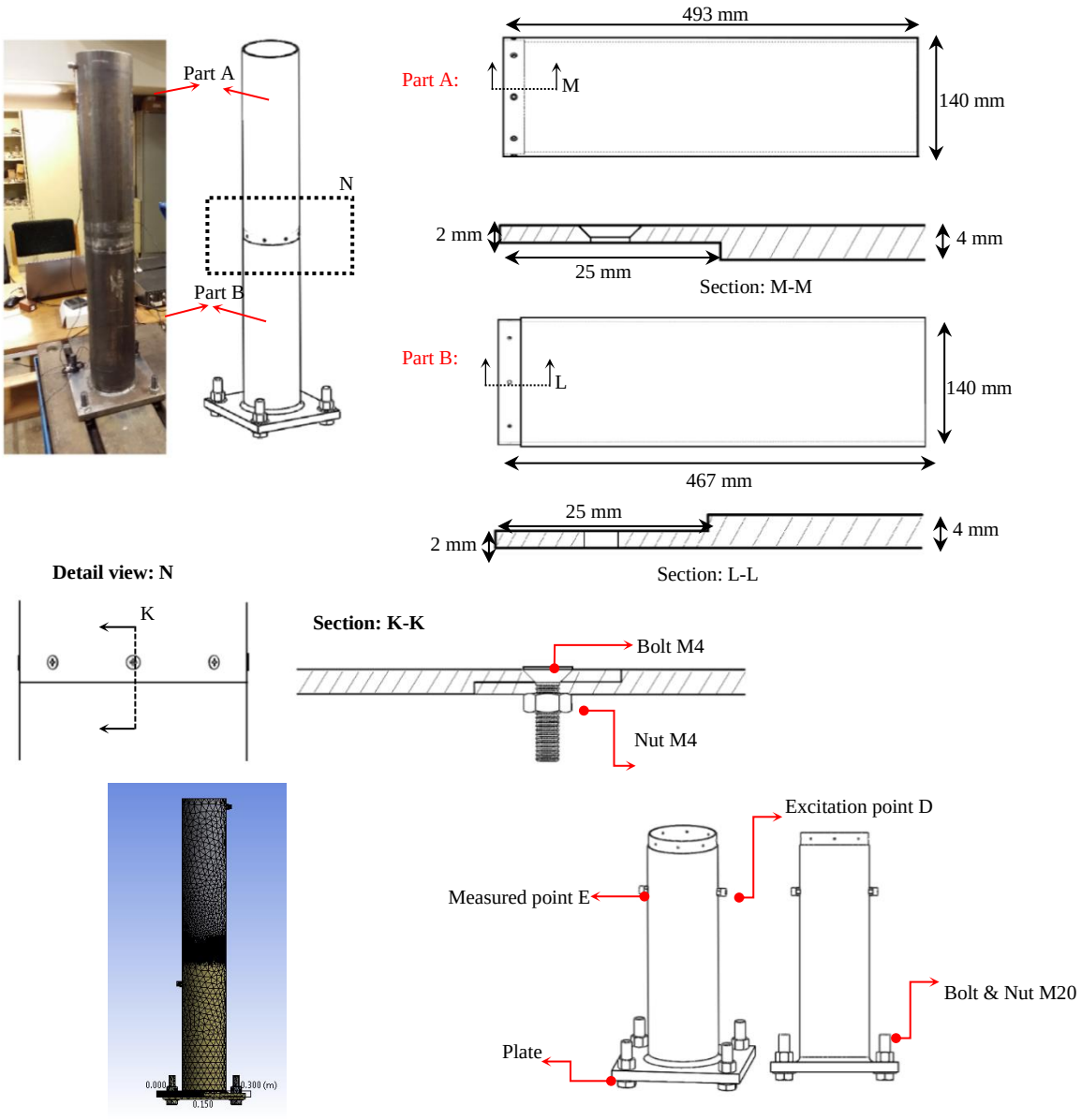

Fig. 3: Details of the test structure and associated FE model

The substructure bending modes are sensitive to the elastic support stiffness; therefore, measurement points were selected away from its upper edge to be able to capture the bending modes and not just the shell oval modes. Preload of M20 bolts, used to ground the structure, was set in a manner that the natural frequencies of the structure were insensitive to its perturbations. The effect of fixed boundary condition was verified by increasing the preload and exciting the structure by the hammer in a second test. It is worth mentioning that a tightening torque of 220 N.m produced the preload in the bolts. As shown in Figure 4, the sub-structure B inertance was insensitive to the variation of preload applied on grounding bolts.

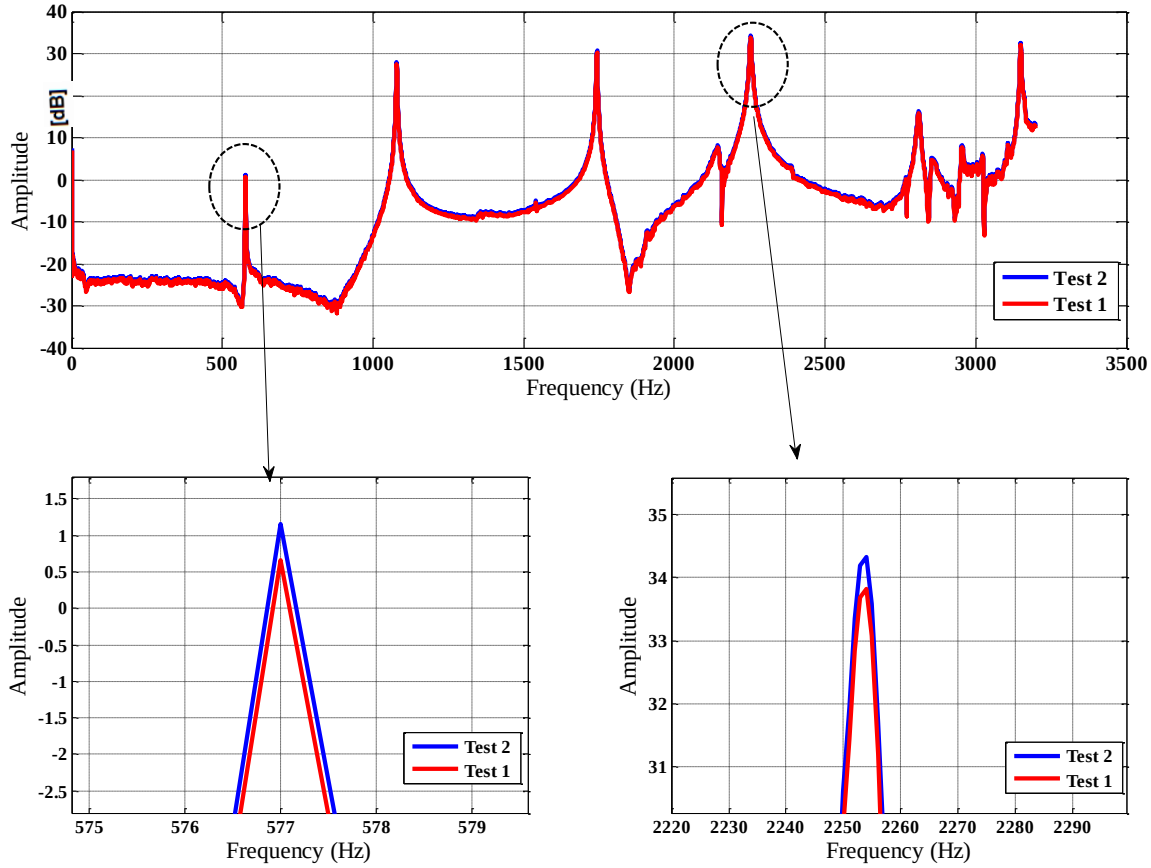

Fig. 4: Linear frequency response function (inertance) of sub-structure B

Next, in order to extract the natural frequencies of the cylindrical structure, the assembled structure is excited by a hammer, as shown in Figure 5(a). The frequency response of the structure is shown in Figure 5(b), and the experimentally measured natural frequencies are tabulated in Table 1.

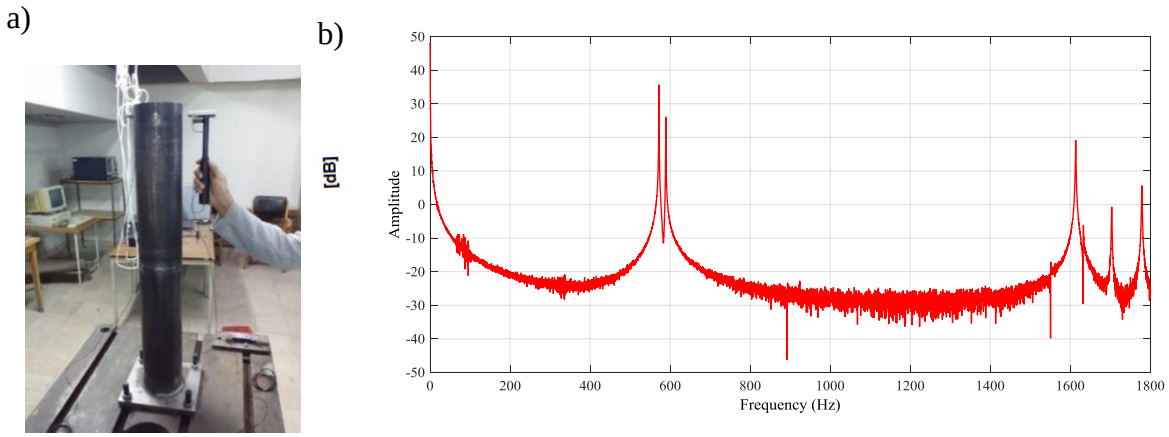

Fig. 5: (a Impact hammer test setup, b) Linear frequency response function of the assembled structure

3.2. Harmonic force excitation

In the next step of the experiments, the cylindrical structure was excited by harmonic forces. The assembled structure was excited at point B by an electromagnetic shaker to determine the nonlinear characteristics of the joint contact. The system response was recorded at point C by an accelerometer to achieve a response with high signal to noise ratio; the measurement points and the test setup are shown in Figure 6. The excitation point was selected at point B near the contact to reduce the amplitude of the electromagnetic shaker movement. Nonlinear effects of the shaker magnetic field due to the large displacement of its armature are minimized by careful selection of excitation point, and mainly the nonlinear effects of the contact are recorded.

The type of excitation in this section was single harmonic, unlike the previous tests which were performed to determine the linear characteristics of the system. The excitation frequencies were selected near the first resonance frequency of structure to achieve high response amplitudes with minimum efforts. The structure was excited under constant amplitude harmonic loading at specified frequencies near its first resonance frequency to find its nonlinear response, and its steady-state responses were recorded versus time.

During shaker tests with high input force, the structure showed strong nonlinear behavior, and the response signal contained higher harmonics. It is due to the fact that the actual force applied to the structure under test was the reaction force between the exciter and the structure. There are many algorithms to control the shaker and cancel the undesired harmonics of the force signal. Using a straightforward algorithm, the overall error for the amplitude of undesired force harmonics is set to 1 percent of the fundamental harmonics.

Considering the response of the cylindrical structure includes the principal harmonic of excitation and its multiples, the amplitude of the principal harmonic was determined from the experimental results by Fourier series expansions of the structure time response. The nonlinear frequency responses under different harmonic load levels in the vicinity of the first resonance of the structure obtained from the experimental results are shown in Figure 7. The selected

excitation force levels were able to excite the nonlinear effects of the structure and cause resonance frequency shift due to the occurrence of micro-slip phenomenon in the contact region. The structure shows softening effects at higher excitation amplitude. The fundamental resonance frequency of the structure obtained in low-level excitation forces using hammer tests was 571.61 Hz. There was not much shift in the resonance frequency in proceeding experiments until the force level exceeds 9N. In Fig 7, it is evident that at 9N level of excitation, the resonance frequency is still 571.6, and the obtained FRF is symmetric about the resonance frequency indicating linear behavior of the assembled structure.

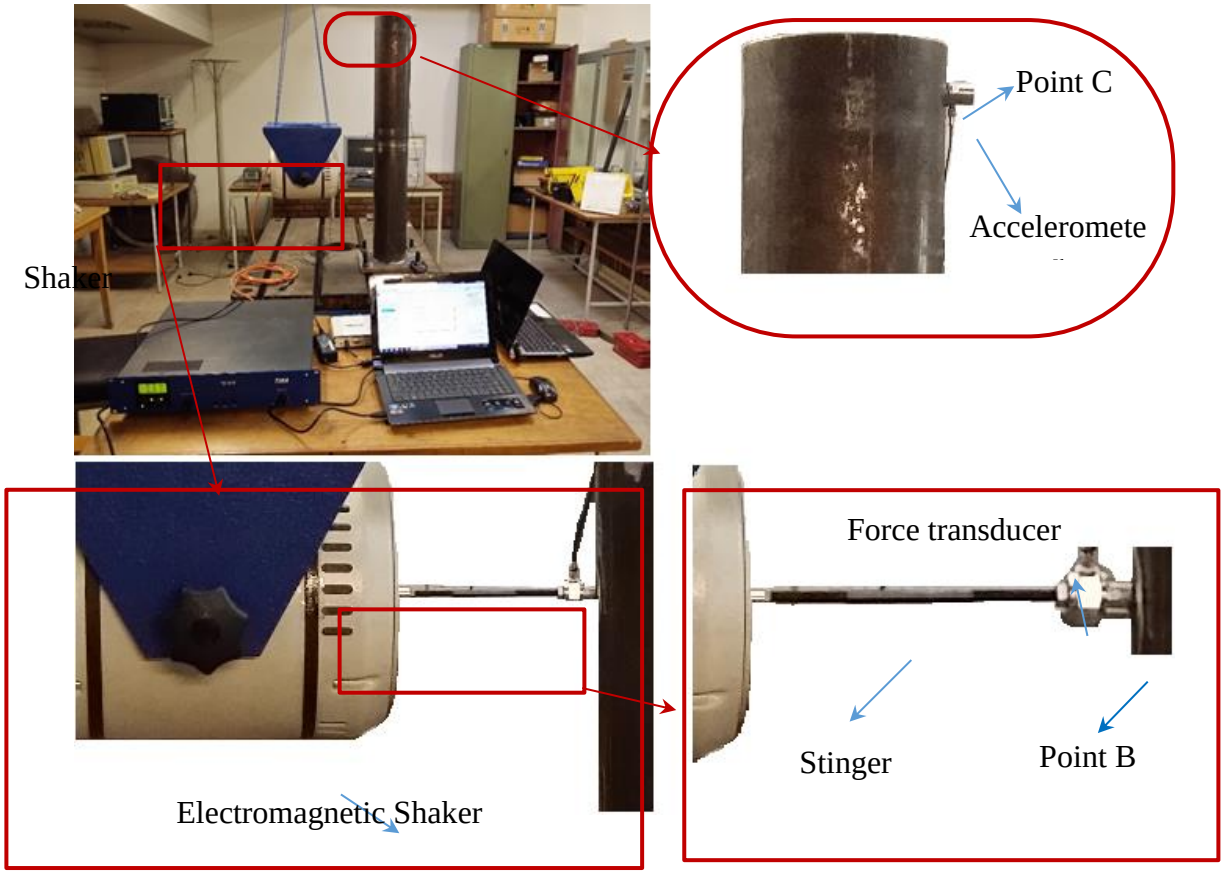

Fig. 6: Harmonic excitation test setup

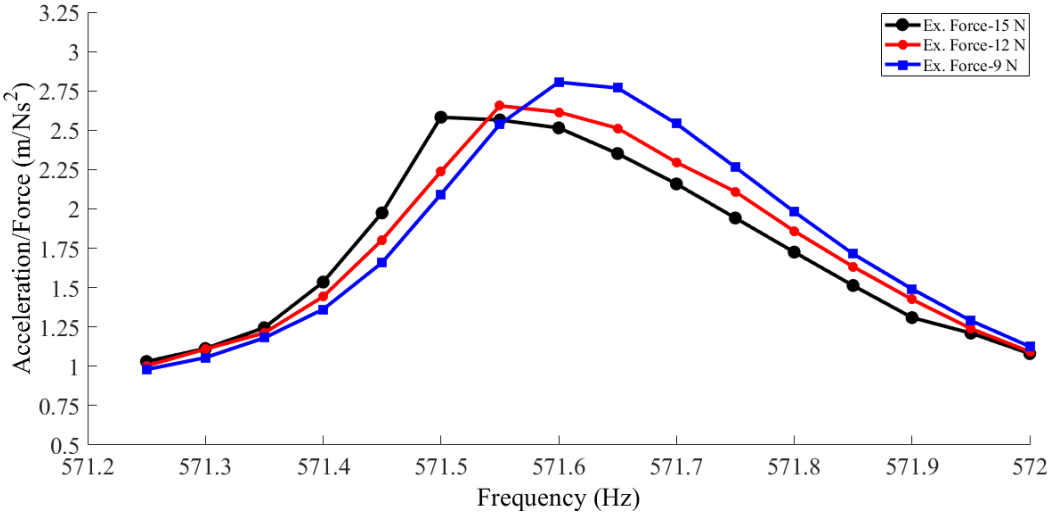

Fig. 7: Nonlinear frequency response functions at different excitation force levels

At higher levels of excitations, i.e., 12N and 15N, shifts occur in the resonance frequencies. Nonlinear characteristics of the structure with softening effects are observed in corresponding measured frequency responses as follows,

- The shift in resonance frequency is evident in figure (7); as the excitation amplitude increases, the resonance frequency reduces in a monotonic manner.
- The jump phenomenon in the frequency response is produced as the nonlinear mechanisms become active in the structure at higher excitation amplitudes. The measured frequency responses at higher excitation amplitude are not symmetric about resonance point, and they lean to the left (lower frequencies), indicating the occurrence of jump phenomena in frequency responses.
- As excitation amplitude increases, the micro/macro slip mechanisms become active in the contact interface leading to an increase in the modal damping. An increase in the modal damping is evident in figure (7), where the amplitude of response at resonance frequency decreases at higher excitation amplitudes.

4. Joint model identification

The joint interface model has two sets of parameters; the first set defines its normal and tangential stiffness at stick state while the second set of parameters defines micro/macro-slip behavior of the contact. The first set of parameters are updated using modal tests performed at low excitation amplitudes, where the structure behaves linearly. Next, nonlinear vibration behavior of the structure at higher amplitudes is employed to determine the second set of parameters. It is worth mentioning that the uncertainty in FE models of substructures was reduced by performing model validation against measured modes of each substructure before updating the contact interface parameters. Therefore in the assembled FE model, shown in Fig. 3, the unknowns are joint interface parameters that are identified in the following.

4.1. Linear model updating

In this step, using experimental data obtained at low excitation force with linear behavior of the joint, the stiffness parameter of each model at the sticking state is updated. For thin layer interface model, parameters $E_e$and υ are updated while the mass density of the layer is set to a small value ($1\ \frac{\mathrm{kg}}{\mathrm{m}^3}$). In the zero thickness contact model, tangential stiffness at both directions are assumed equal and normal and tangential stiffness, i.e. K_n and K_t, are updated. To specify E_e and υ in thin layer model and normal and tangential stiffness of zero thickness model, an objective function is defined as:

$$\min \sum_{i=1}^{j} W_i \left(\frac{\left| f_{EXP_i} - f_{FEM_i} \right|}{f_{EXP_i}} \right) \tag{9}$$

In Eqn. (9), W_i is a real positive weighting factor, f_{FEM_i} is predicted resonance frequency, determined from the finite element model and f_{EXP_i} is experimentally measured resonance frequency obtained from hammer tests performed on the structure. The number of resonance frequencies employed in the updating practice, *j*, equals to 3 as the first three modes within the measurement range were sensitive to the contact interface parameters. The linear updating process of FE models was performed using Particle Swarm Optimization (PSO). A comparison between the first three natural frequencies of the structure determined from the updated models and results of the experimental test, as presented in Table 1, shows the success of both models in the updating process. The resulting updated values of E_e, υ, K_n and K_t are presented in Table 2, respectively. Also, in Figures 8-9, the trend of changes in the objective function and linear contact parameters are shown during the optimization processes.

Table. 1: Experimental and updated natural frequencies

	$f_1(Hz)$	Error (%)	$f_2(Hz)$	Error (%)	$f_3(Hz)$	Error (%)
EXP	571.6113		589.0013		1613.309	
Zero thickness element	572.5033	0.16	586.5596	-0.41	1634.4803	1.31
Thin layer element	576.0524	0.78	596.2671	1.23	1653.1058	2.47

The measure of success in the linear model updating practice is reproducing the experimental observations. The achieved correlations between model predictions and experimental observations are due to two crucial facts: a) the selected class of model in updating practice is an accurate representation of the structure, and b) the employed optimization algorithm, PSO, finds

Table. 2: Identified linear parameters

Zero thickness element		Thin layer theory	
K_t (Pa)	K_n (Pa)	E_e (Pa)	$\boldsymbol{\upsilon}$
1.538 E+13	4.303 E+14	1.88e+11	0.3

the global minimum of the objective function and is not dependent on the initial values of design parameters.

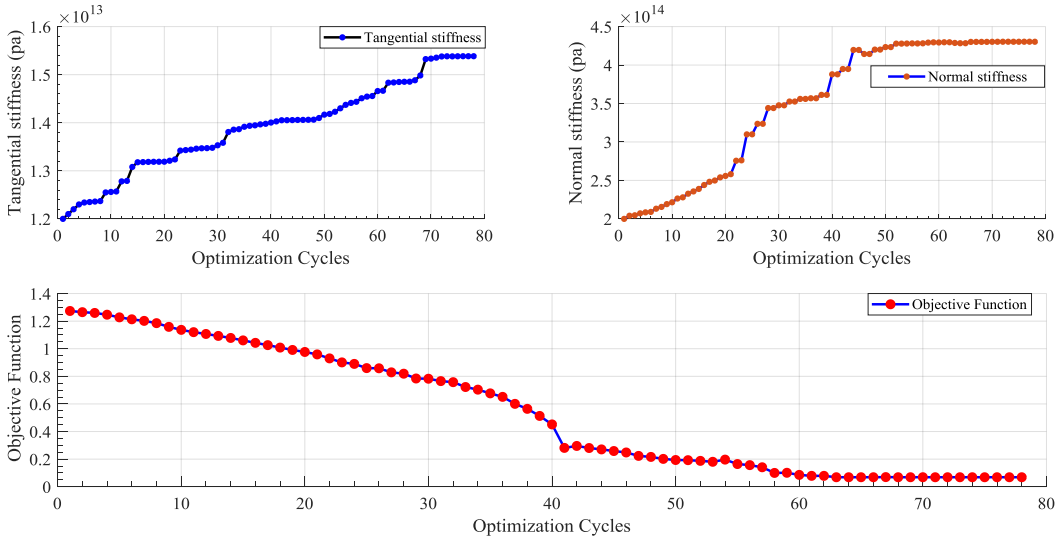

Fig. 8: The objective function and the variations of the joint parameters in the optimization process of zero thickness elements

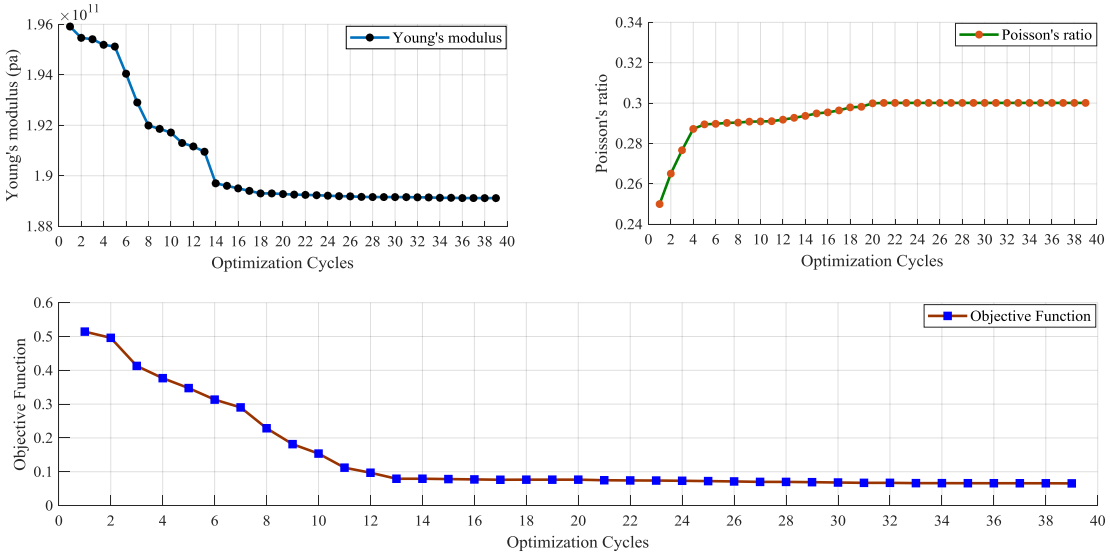

Fig. 9: Variations in the objective function and the joint parameters during the optimization process in thin layer elements

4.2. Nonlinear model updating

In order to identify the nonlinear effects in the bolted lap joint, a nonlinear model updating was also performed. In the nonlinear behavior of the assembled structure, friction plays a significant role in the joint dynamics. The joint interface modeled using zero thickness elements has contact stiffness's which behaves linearly, and the nonlinear effects are modeled using the frictional coefficient μ. In thin layer theory, considering Eqn. (8), E_p, S_y and n represent the nonlinear behavior of the contact region. The parametersE_p, S_y and n determine the macro-slip stiffness, micro-slip limit, and smoothness of transition from stick to macro-slip behavior, respectively. Since results of nonlinear response are functions of the magnitude of the force applied on the structure, the results of the highest amplitude of excitation force, 15N, which creates the highest nonlinear effect in the contact region, were used for estimating the contact parameters. The results pertinent to the other excitation amplitudes were used in order to verify the updated model capability in predicting observation not used in parameter estimations. The process of optimization to update the parameters of frictional contact in the FE model was done using the PSO method in which the contact parameters were defined as design variables. As the PSO method arrives at its final parameter values in fewer generations compared to other methods [30], this method was used for updating the nonlinear parameter of both thin layer interface and zero thickness elements.

The model response estimations are performed for the frequencies within the range of the first resonance of structure and highest excitation force amplitude in the experimental test. The results from FE analyses and experimental tests are employed for calculating the objective function in the optimization process. The objective function in this optimization process was defined as the magnitude of the relative difference in the results of the response amplitudes, χ, in the corresponding frequency:

$$\min \sum_{i=1}^{j} \overline{W_i} \left(\frac{|\chi_{EXP} - \chi_{FEM}|}{\chi_{EXP}} \right). \tag{10}$$

In equation (10), $\overline{W_i}$ is a real positive weighting factor, χ_{EXP} is the nonlinear experimental frequency response amplitude, χ_{FEM} is the nonlinear frequency response amplitude of the finite element model, and ' j ' is the number of selected frequencies used for updating. Figures 10-11 show the trend of changes in the objective functions and frictional contact parameters during the optimization processes. The updated value of μ, E_p, S_y and n are presented in Table 3.

Table. 3: Identified nonlinear parameters

Zero thickness parameter	Thin layer parameters		
μ	E_p(Pa)	S_y(Pa)	$\boldsymbol{n}$
0.5440458	**9.783e+07**	**1.129 e+08**	2.153

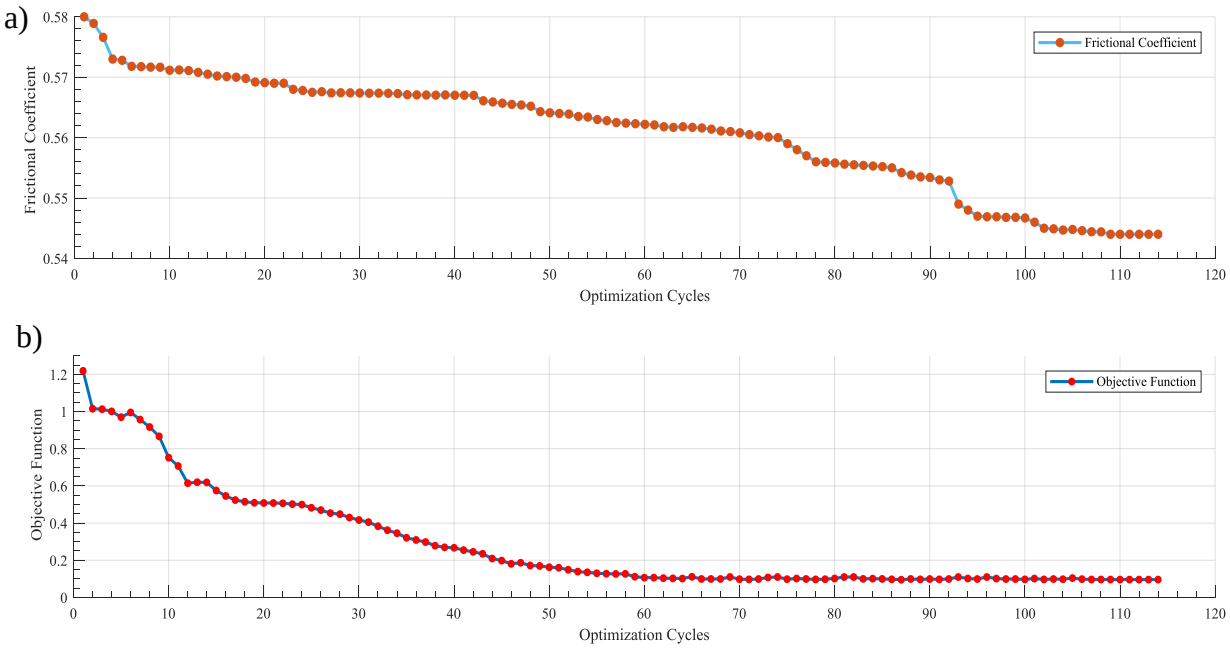

Fig. 10: (a Frictional coefficient b) Changes in the objective function

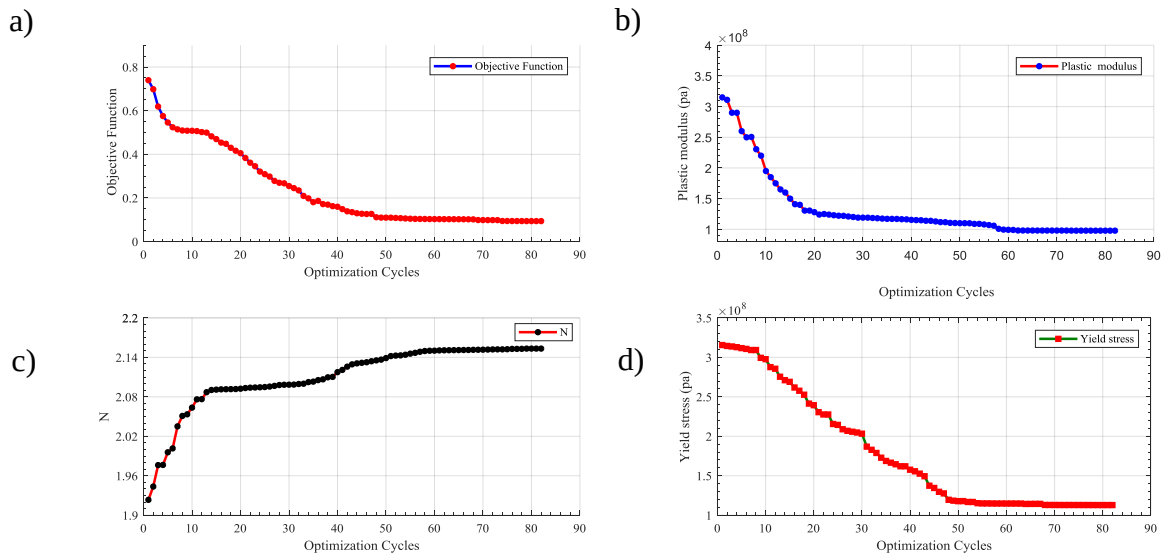

Fig. 2: Thin layer parameters a) Changes in the objective function b) Plastic modulus c) n (Smoothness of transition) d) Yield stress

5. Model verification

In the previous steps, FE model parameters were updated using the experimental results. These parameters were obtained using one set of experimental data with a specified excitation force. A comparison between experimental results and the FE model with updated contact parameters for the amplitude of the 15N excitation force is depicted in Figure 12. This figure shows the ratio of acceleration to excitation force principal harmonics vs. the excitation frequency.

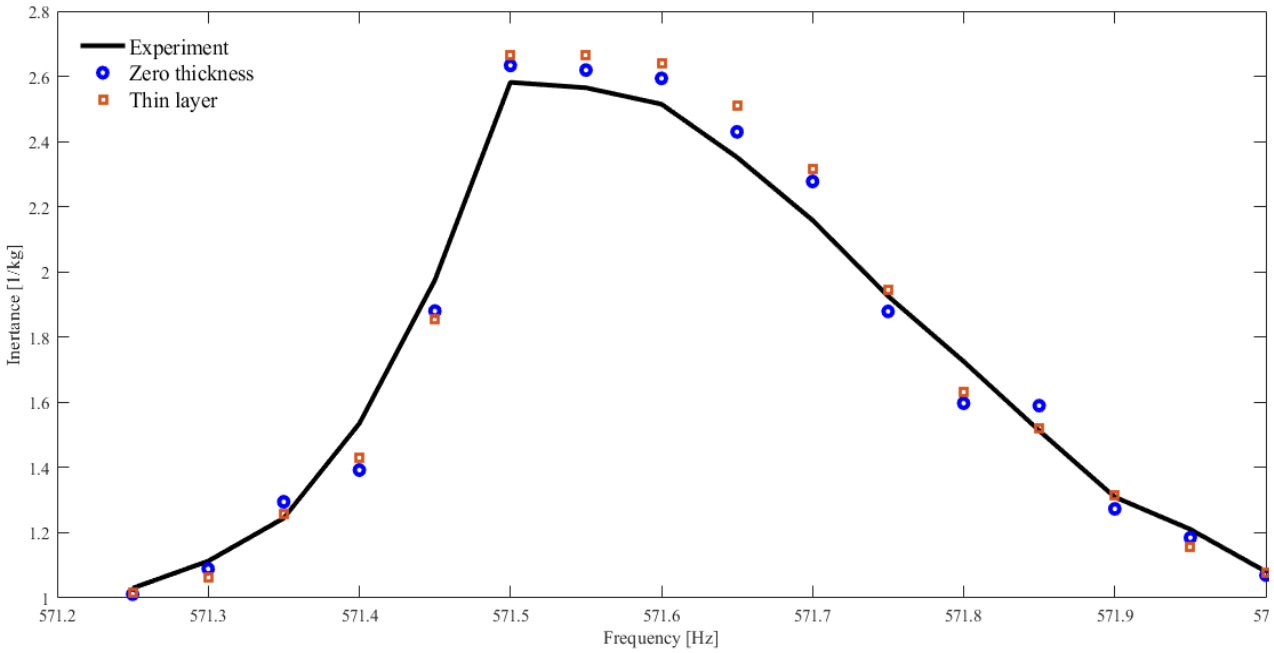

Fig. 12: Measured and updated model FRFs, excitation force of 15N

In order to verify the validity of the model, its predictions against experimental results in other excitation amplitudes, i.e., 12N and 9N, were also considered. In Figure 13, a comparison of the prediction results from both models and experimental FRFs with the amplitude of the excitation forces of 12N and 9N are shown. According to Figure 13, there is a good concordance between the results from the identified FE models and the results from the experimental test.

Another means of verifying the identified model is the comparison between hysteresis loops, which are predicted from the FE model, and similar curves resulted from the test. Figure 14 compares the force-acceleration hysteresis loops related to the identified model and the experimental results in the frequency of 571.5 Hz and the excitation force of 15N.

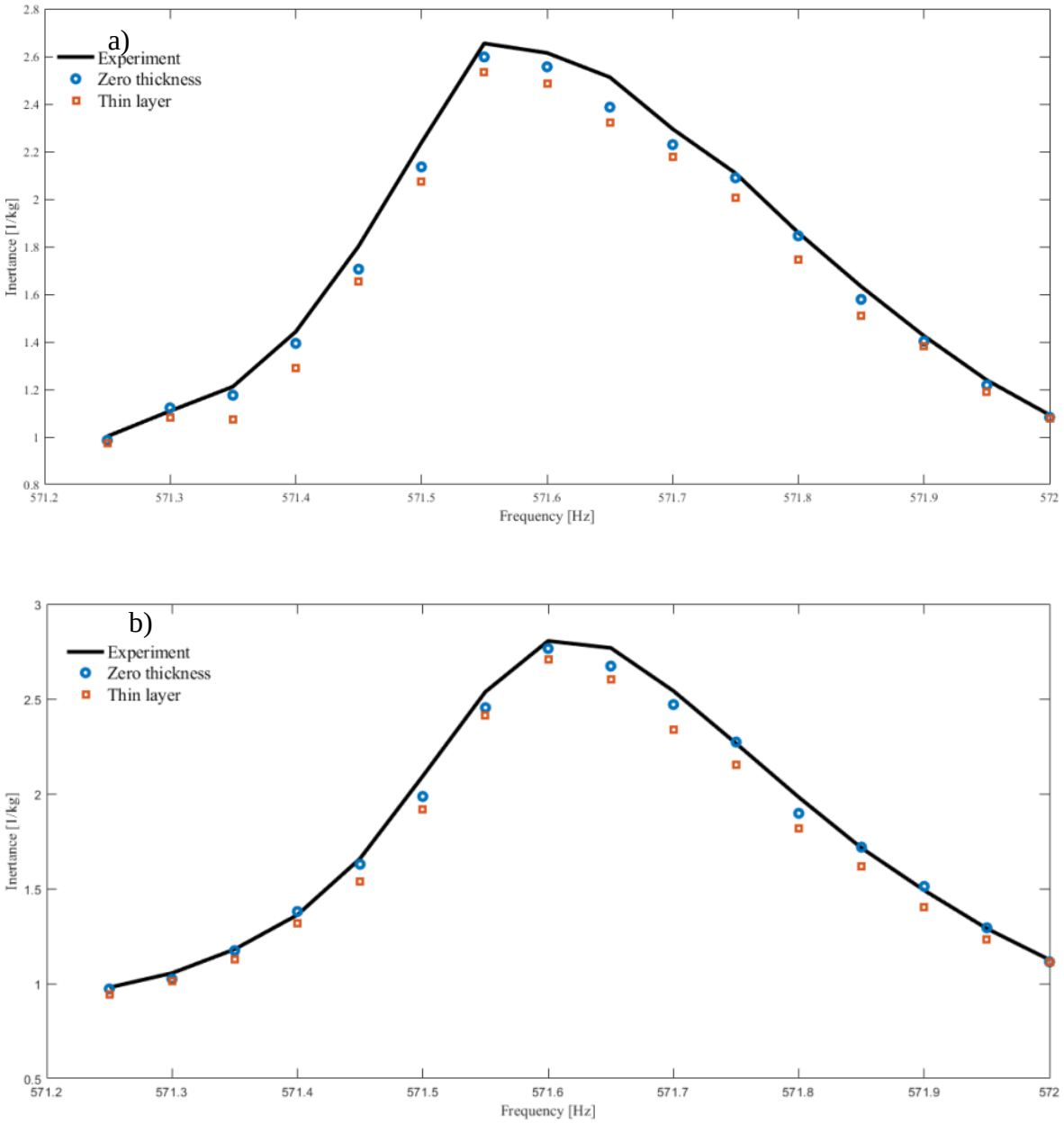

Fig .3: The measured data and predicted responses, a) excitation force 12N, b) excitation force 9 N.

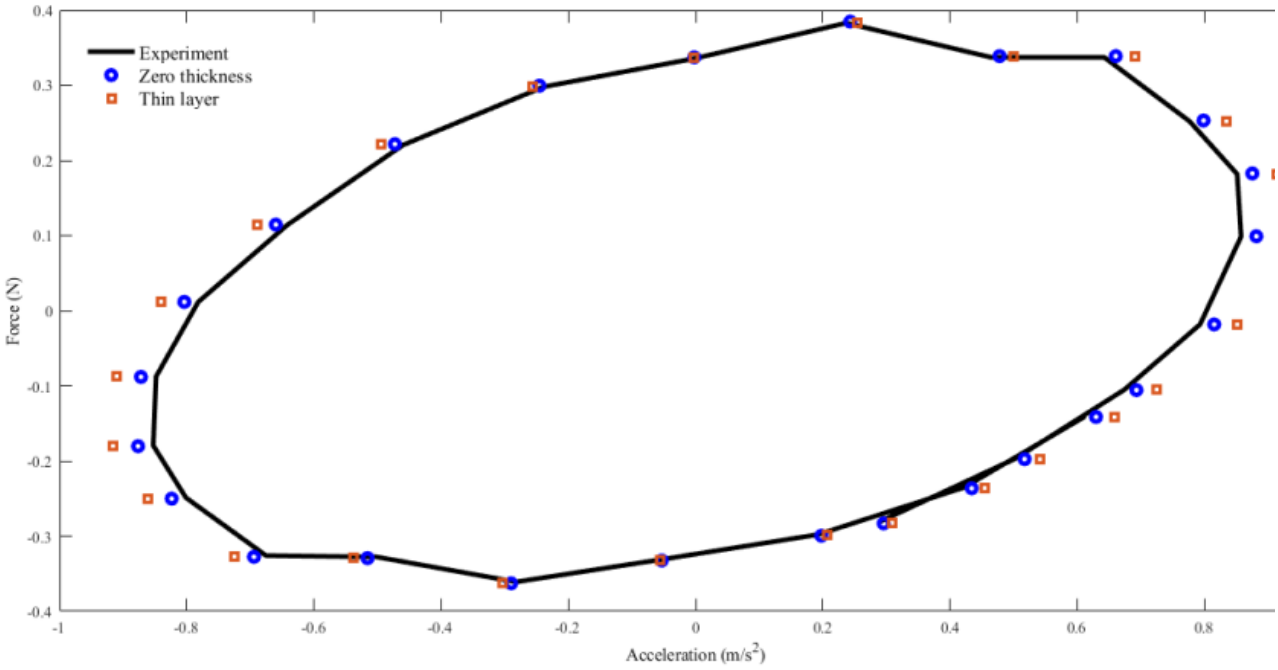

Fig. 4: The measured and predicted hysteresis loops at 571.5 Hz with excitation amplitude of 15N

The comparisons between the two contact models predictions and experimental hysteresis loops at other excitation forces are shown in Figure 15. As the normal contact force varies in each load cycle, the hysteresis loops take complex shape; however, according to Figure 15, the FE model predicts the results of the experimental test very well. It is worth mentioning the advantage, and also, the primary motivation, of using the thin layer element in modeling lap joint contact is its fast convergence rate in obtaining the nonlinear response of the structure as well as avoiding substantial computational efforts and time-consuming processes compared to the frictional zero thickness element.

The thin layer element is much simpler to generate in the modeling process, and it is in general preferable to the zero thickness element due to,

a) Models involving zero thickness elements produce ordinary differential equations that are numerically stiff and, therefore, computationally cumbersome.

b) A smooth constitutive law such as the one used in the thin layer interface virtual material well represents the lap joints micro/macro slip effects, and the interface model is numerically more efficient.

a)

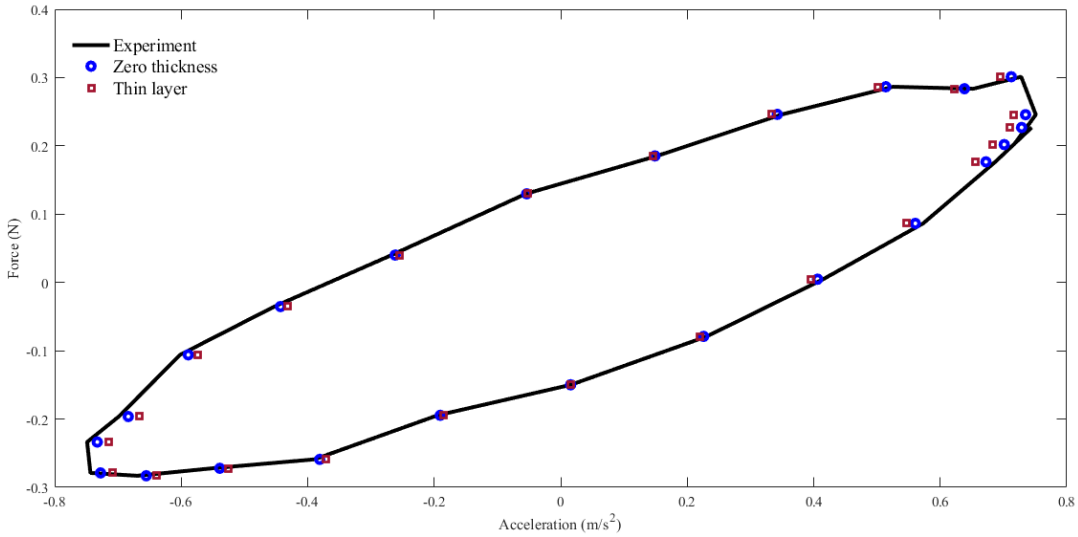

b)

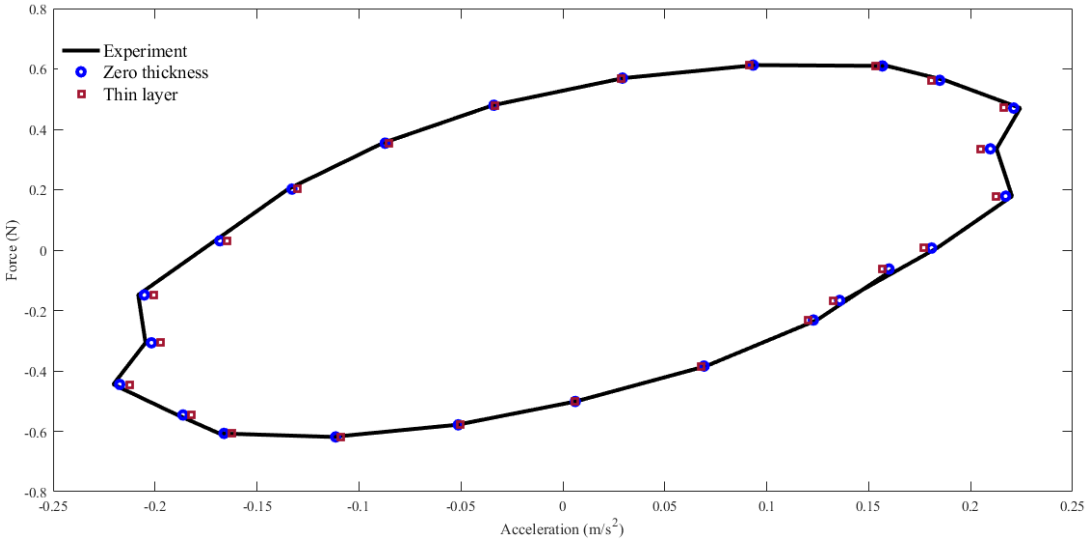

Fig. 5: Measured and predicted hysteresis loops: a) at excitation force of 12N, b) at excitation force of 9N

The comparisons between the two contact models predictions and experimental hysteresis loops at other excitation forces are shown in Figure 15. As the normal contact force varies in each load cycle, the hysteresis loops take complex shape; however, according to Figure 15, the FE model predicts the results of the experimental test very well. It is worth mentioning the advantage, and also, the primary motivation, of using the thin layer element in modeling lap joint contact is its fast convergence rate in obtaining the nonlinear response of the structure as well as avoiding substantial computational efforts and time-consuming processes compared to the frictional zero thickness element.

The thin layer element is much simpler to generate in the modeling process, and it is in general preferable to the zero thickness element due to,

c) Models involving zero thickness elements produce ordinary differential equations that are numerically stiff and, therefore, computationally cumbersome.

d) A smooth constitutive law such as the one used in the thin layer interface virtual material well represents the lap joints micro/macro slip effects, and the interface model is numerically more efficient.

6. Conclusion

In this paper, a comparison between two common strategies of modeling lap joints, namely, zero-thickness and thin layer interface elements, was made. A finite element model capable of accurately representing the dynamic behavior of an assembled structure with localized nonlinearities was developed. The lap joint parameters of the structure were updated to reduce the discrepancies between experimental observations and model predictions. Comparisons with experimental data were performed to validate the developed models, using load cases that were not included in the updating process. In what concerns the updating process, the convergence rate of the contact model with frictional contact element in calculating the dynamic response of structure was lower and required more computations compared to the corresponding thin layer model. This can be explained using the fact that in all considered load cases, the normal load in contact did not approach zero. Hence a smooth constitutive law such as the one used in the thin layer interface virtual material well represented the lap joints nonlinear effects. This removes the need to use penalty methods to distinguish abrupt changes between stick and slip states as employed in the frictional contact model and reduced the computational efforts in obtaining the contact forces. Nevertheless, accurate predictions of nonlinear frequency responses and hysteresis loops proved that both contact models well represent different states of the contact under normal variable loading, which results in complex behavior such as non-smooth hysteresis loops.

References

[1] M.A. Beaudoin, K. Behdinan, Analytical lump model for the nonlinear dynamic response of bolted flanges in aero-engine casings, Mechanical Systems and Signal Processing, 115 (2019) 14-28.
[2] H. Festjens, G. Chevallier, J.L. Dion, Nonlinear model order reduction of jointed structures for dynamic analysis, Journal of Sound and Vibration, 333 (2014) 2100-2113.
[3] C. Stocchi, P. Robinson, S.T. Pinho, A detailed finite element investigation of composite bolted joints with countersunk fasteners, Composites Part A: applied science and manufacturing, 52 (2013) 143-150.
[4] H. Jalali, H.H. Khodaparast, M.I. Friswell, The effect of preload and surface roughness quality on linear joint model parameters, Journal of Sound and Vibration, 447 (2019) 186-204.
[5] S. Daouk, F. Louf, C. Cluzel, O. Dorival, L. Champaney, S. Audebert, Study of the dynamic behavior of a bolted joint under heavy loadings, Journal of Sound and Vibration, 392 (2017) 307-324.
[6] M. Eriten, M. Kurt, G. Luo, D.M. McFarland, L.A. Bergman, A.F. Vakakis, Nonlinear system identification of frictional effects in a beam with a bolted joint connection, Mechanical Systems and Signal Processing, 39 (2013) 245-264.
[7] C. Ehrlich, A. Schmidt, L. Gaul, Reduced thin-layer elements for modeling the nonlinear transfer behavior of bolted joints of automotive engine structures, Archive of Applied Mechanics, 86 (2016) 59-64.
[8] C. Ehrlich, A. Schmidt, L. Gaul, Microslip joint damping prediction using thin-layer elements, in: Dynamics of Coupled Structures, Volume 1, Springer, 2014, pp. 239-244.

[9] M. Iranzad, H. Ahmadian, Identification of nonlinear bolted lap joint models, Computers & Structures, 96 (2012) 1-8.
[10] H. Jalali, A. Hedayati, H. Ahmadian, Modelling mechanical interfaces experiencing micro-slip/slap, Inverse Problems in Science and Engineering, 19 (2011) 751-764.
[11] M.M. Alamdari, J. Li, B. Samali, H. Ahmadian, A. Naghavi, Nonlinear joint model updating in assembled structures, Journal of Engineering Mechanics, 140 (2014) 04014042.
[12] B.J. Deaner, M.S. Allen, M.J. Starr, D.J. Segalman, H. Sumali, Application of viscous and Iwan modal damping models to experimental measurements from bolted structures, Journal of Vibration and Acoustics, 137 (2015).
[13] R.M. Lacayo, B.J. Deaner, M.S. Allen, A numerical study on the limitations of modal Iwan models for impulsive excitations, Journal of Sound and Vibration, 390 (2017) 118-140.
[14] R.M. Lacayo, M.S. Allen, Updating structural models containing nonlinear Iwan joints using quasi-static modal analysis, Mechanical systems and signal processing, 118 (2019) 133-157.
[15] J. Abad, F.J. Medel, J.M. Franco, Determination of Valanis model parameters in a bolted lap joint: Experimental and numerical analyses of frictional dissipation, International Journal of Mechanical Sciences, 89 (2014) 289-298.
[16] D.J. Segalman, Modelling joint friction in structural dynamics, Structural Control and Health Monitoring: The Official Journal of the International Association for Structural Control and Monitoring and of the European Association for the Control of Structures, 13 (2006) 430-453.
[17] E.J. Berger, Friction modeling for dynamic system simulation, Appl. Mech. Rev., 55 (2002) 535-577.
[18] H. Ahmadian, H. Jalali, Generic element formulation for modelling bolted lap joints, Mechanical Systems and Signal Processing, 21 (2007) 2318-2334.
[19] M.J. Mashayekhi, J. Kövecses, A comparative study between the augmented Lagrangian method and the complementarity approach for modeling the contact problem, Multibody System Dynamics, 40 (2017) 327-345.
[20] G. Stadler, Path-following and augmented Lagrangian methods for contact problems in linear elasticity, Journal of computational and applied mathematics, 203 (2007) 533-547.
[21] S. Stupkiewicz, J. Lengiewicz, J. Korelc, Sensitivity analysis for frictional contact problems in the augmented Lagrangian formulation, Computer methods in applied mechanics and engineering, 199 (2010) 2165-2176.
[22] R. Lacayo, L. Pesaresi, J. Groß, D. Fochler, J. Armand, L. Salles, C. Schwingshackl, M.S. Allen, M. Brake, Nonlinear modeling of structures with bolted joints: a comparison of two approaches based on a time-domain and frequency-domain solver, Mechanical Systems and Signal Processing, 114 (2019) 413-438.
[23] M. Sanati, Y. Terashima, E. Shamoto, S.S. Park, Development of a new method for joint damping identification in a bolted lap joint, Journal of Mechanical Science and Technology, 32 (2018) 1975-1983.
[24] Z. Qin, D. Cui, S. Yan, F. Chu, Application of 2D finite element model for nonlinear dynamic analysis of clamp band joint, Journal of Vibration and Control, 23 (2017) 1480-1494.
[25] J. Abad, J.M. Franco, R. Celorrio, L. Lezáun, Design of experiments and energy dissipation analysis for a contact mechanics 3D model of frictional bolted lap joints, Advances in Engineering Software, 45 (2012) 42-53.
[26] E. Pennestrì, V. Rossi, P. Salvini, P.P. Valentini, Review and comparison of dry friction force models, Nonlinear dynamics, 83 (2016) 1785-1801.
[27] C.S. Desai, M.M. Zaman, J.G. Lightner, H.J. Siriwardane, Thin-layer element for interfaces and joints, International Journal for Numerical and Analytical Methods in Geomechanics, 8 (1984) 19-43.
[28] G.N. Pande, K.G. Sharma, On joint/interface elements and associated problems of numerical ill-conditioning, International Journal for Numerical and Analytical Methods in Geomechanics, 3 (1979) 293-300.
[29] M.H. Mayer, L. Gaul, Segment-to-segment contact elements for modelling joint interfaces in finite element analysis, Mechanical systems and signal processing, 21 (2007) 724-734.
[30] S. Panda, N.P. Padhy, Comparison of particle swarm optimization and genetic algorithm for FACTS-based controller design, Applied soft computing, 8 (2008) 1418-1427.